Dynamical behavior of the exciton polariton in CuCl: Coherent propagation and momentum relaxation

T. Ikehara and T. Itoh
Department of Physics, Faculty of Science, Tohoku University, Sendai 980, Japan
(Received 22 March 1991)

Exciton-polariton luminescence spectra in CuCl single crystals of high purity are investigated at 2 K using picosecond time-resolved spectroscopy with high temporal and spectral resolutions. The excitation density is kept in the weak-excitation regime. Experimental results are analyzed in the "polariton-picture" framework for the exciton-photon system. Under excitation well above the lowest exciton energy, the intraband relaxation and the bottleneck effect of the polaritons are clearly manifested in the 2-LO-phonon replica of the exciton luminescence. On the other hand, pulsed responses are found in the polariton resonant luminescence near the transverse-exciton energy. The coherent propagation of polaritons and their radiative escape from the crystal surface produce the pulsed responses in the luminescence while they propagate to and fro between the front and the rear surfaces of the slab sample. They propagate for a distance of more than 20 μm. The momentum-relaxation probability per unit time is evaluated as a function of the energy from the intensity ratio of successive pulsed responses of the resonant luminescence. It varies from 10^9 s^{-1} near the transverse-exciton energy up to 10^{10} s^{-1} near the longitudinal-exciton energy. The sample dependence of the polariton luminescence spectra is also elucidated by the competitive relation between the lifetime, propagation time, and the intraband relaxation time of the polaritons. The discrepancy between the transmission spectrum calculated from the momentum-relaxation probability and that obtained experimentally is discussed. This discrepancy is associated with the strong effect that very fine surface roughness may have on the transmission spectrum.

I. INTRODUCTION

The exciton polariton (EP) is an eigenstate for the exciton-photon system in semiconductor crystals when the interaction of an exciton with a photon is strong enough compared with other interactions.[1,2] The dispersion relation of the EP at energy E and wave vector k is represented by

$$\frac{\hbar^2c^2k^2}{E^2}=\epsilon_b\frac{[E_L+(\hbar^2k^2/2m_{ex})]^2-E^2}{[E_T+(\hbar^2k^2/2m_{ex})]^2-E^2}\ , \tag{1}$$

where E_T, E_L, m_{ex}, and ϵ_b are the energies of transverse and longitudinal excitons, the translational exciton mass, and the background dielectric constant, respectively. For simplicity in Eq. (1) no damping process is included.

If there exist no other perturbations, the EP has infinite lifetime in itself. Therefore, in order to understand the actual behavior of the EP, it is essential to study the dynamics of the EP including the interactions with phonons and crystal defects. Many theoretical studies on the relaxation mechanism of the EP have been performed in the past 30 years. Hopfield showed the existence of the EP and pointed out the importance of the interaction with phonons.[1] Toyozawa[3,4] and Sumi[5] investigated exciton-phonon interactions and discussed the radiative decay of the EP. They showed the EP population exhibits an accumulation around the transverse-exciton energy due to the detailed balance of the acoustic phonon scattering and the radiative decay. This has been well known as a "bottleneck effect."

The development of ps time-resolved spectroscopy has made it possible to study the dynamics of the EP experimentally. The energy relaxation processes of the EP distributed widely on the dispersion curve have been studied in CdS,[6] CuCl,[7] and CdSe (Ref. 8) by observing the ps time-resolved spectra of the exciton resonant luminescence, the induced absorption from the EP state to the excitonic molecule state, and the phonon sideband luminescence, respectively. However, most of the previous experiments with the use of ps time-resolved spectroscopy could not directly show the detailed dynamics of the EP, such as phonon or impurity scattering, radiative decay, and dynamical behavior in real space. For example, the spatial dynamics of the EP has usually been treated by a diffusion equation in the analysis of the exciton luminescence. However, it is also known from time-of-flight measurements[9,10] that the EP can propagate coherently over some distance with a group velocity v_g, which may be calculated by using the dispersion relation [Eq. (1)] and the following relation:

$$v_g(E)=\frac{1}{\hbar}\frac{dE}{dk}\ . \tag{2}$$

Which picture, coherent or incoherent motion, is more realistic for the dynamics of the EP? It should depend on the scattering rate of the EP. Besides, the existence of elastic scattering by crystal imperfections has been inferred by several authors in order to explain the transmission spectrum,[11] resonant Brillouin scattering,[12] and luminescence line shape near the exciton resonance.[13] However, no direct method has been established so far on how to evaluate the elastic-scattering probability.

There were several reasons why one failed, in the previous time-resolved experiments, to observe the detailed dynamics of the EP: (1) Due to a high peak intensity of the excitation light pulse, high-density excitation effects were inevitable, for example, EP-EP collision, formation of excitonic molecules, induced absorption from the exciton state to the excitonic molecule state. These effects disturbed the original nature of the EP. (2) The time resolution and/or the spectral resolution in the experiments were insufficient because of a poor signal-to-noise ratio. (3) Although the dynamics of the EP is quite sensitively affected by the existence of impurities and defects, it was difficult to distinguish the intrinsic nature from the extrinsic one.

Afterward, by solving the above problems, some authors reported experimental efforts for the investigation of intrinsic dynamics of EP's and excitons in anthracene[14,15] and GaAs.[16–18] However, because of the very large exciton effective mass in anthracene and the very small polariton effect in GaAs, the essential nature of the EP has been mostly unknown.

Being different from the above-mentioned situation, the exciton in CuCl has a large spatial dispersion effect and a large oscillator strength. Therefore, the exciton clearly shows both the Wannier-exciton nature and the polariton nature. The dispersion relation given by Eq. (1) for the Z_3 exciton in CuCl is shown in Fig. 1(a) with the following parameters: $E_T=3.202\,23$ eV, $E_L=3.207\,88$ eV, $m_{ex}=2.3m_0$ (m_0 is the electron mass in vacuum), and $\epsilon_b=5.59$.[19] The group velocity $v_g(E)$ calculated from Eq. (2) is also shown in Fig. 1(b) by a solid line for the lower-branch EP. It has been known that these theoretical formulas well represent the experimental results around the exciton resonance energy.[10,20] We have recently succeeded in investigating the time-resolved intrinsic luminescences associated with the EP in ultrapure single crystals of CuCl at 2 K, with high temporal and spectral resolutions and without any effects of high-intensity excitation.[21,22] In our previous reports, we have found pulselike structures in the temporal responses of the resonant luminescence of the EP under the excitation at the second ($Z_{1,2}$) exciton absorption band by weak ps uv light pulses. We have shown that a large number of the EP's at the Z_3 exciton resonance region propagate coherently with their group velocity for a distance of more than 20 μm without being affected by any scattering. Consequently, the spatial inhomogeneity of the distribution of the EP's inside the sample and their coherent propagation have been concluded to be essentially important for the analysis of the resonant luminescence of the EP. This fact clearly shows that the "polariton picture" for the exciton system is actually realized; that is, (1) the EP propagates coherently in the crystal as a wave packet with its group velocity even if it is indirectly generated after multiple phonon scattering, and (2) the EP decays radiatively with a certain probability only when the EP impinges upon the crystal surface.

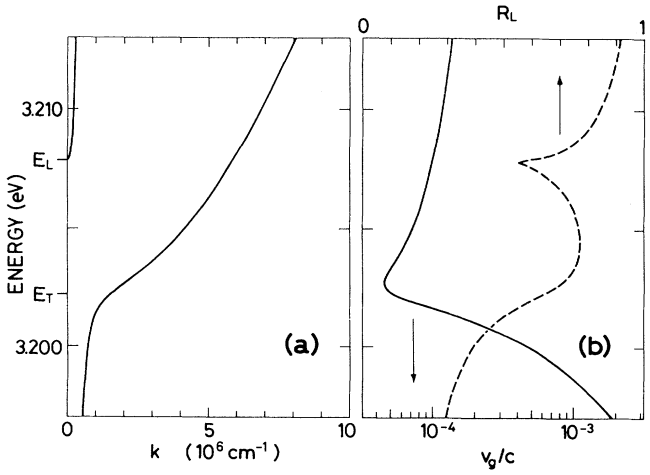

FIG. 1. (a) Dispersion relation of the exciton polariton around the Z_3 exciton energy in CuCl calculated from Eq. (1), where $E_T=3.202\,23$ eV, $E_L=3.207\,88$ eV, $m_{ex}=2.3m_0$, and $\epsilon_b=5.59$. (b) Energy dependences of inside reflectivity $R_L(E)$ (dashed line) and group velocity $v_g(E)$ (solid line) for the lower-branch polariton at the corresponding energy region.

In this paper, we report the temporal behavior of EP luminescences in detail and, furthermore, show that the scattering probability of EP's at each energy can be derived directly from the time-resolved luminescence spectra. This paper consists of the following sections: In Sec. II, we describe experimental procedures for the ps time-resolved spectroscopy with high temporal and spectral resolutions. In Sec. III A, we show that the energy relaxation and the bottleneck effect of the EP show up clearly on the 2-LO-phonon replica (hereafter called the Ex-2LO luminescence). In Sec. III B, we show how the EP propagation modifies the temporal response of the polariton resonant luminescence (Ex luminescence). In Sec. III C, we demonstrate what is essential to determine the line shape of the Ex luminescence. In Sec. III D, we illustrate how the lifetime of the EP modifies the time-integrated EP luminescences. In Sec. III E, we derive the energy-dependent momentum-relaxation rate from the pulsed response of the Ex luminescence. Finally, in Sec. III F, we mention the outward inconsistency of the obtained scattering probability with the transmission spectrum.

II. EXPERIMENTAL PROCEDURES

The material of CuCl was purified from 99%-purity powder by vacuum sublimation and zone-melting methods. Single crystals of CuCl were grown from the vapor phase by taking about 1 week under the atmosphere of H_2 or Ar in a sealed quartz tube. Careful attention was paid not to contaminate the purified materials and the single crystals, in particular, not to be exposed to humidity. The obtained single crystals were platelets with thicknesses ranging from 10 to 20 μm and a diameter of several mm. We evaluated the thickness of each sample from the interference pattern of the transmission spectra in the transparent energy region by taking the polariton dispersion into account. We assessed the purity of the samples on the basis of the lifetime of the EP, the absolute intensities of the EP luminescences, and the inten-

sities of impurity luminescences relative to that of the EP luminescences. We used several samples of different qualities and, therefore, in each figure of this paper we indicated the identification number of the sample and its thickness to clarify the difference. Each sample was carefully put in a small paper bag without any strain and immersed directly into superfluid helium. The paper bag had a small hole at the center acting as a mask in order to prevent the observation of any luminescence from the edge of the sample. All the experiments were performed at 2 K.

We obtained a ps uv light source from a $LiIO_3$ SHG crystal by doubling the light frequency of a pyridine 2 dye laser synchronously pumped by the second harmonic light of a cw mode-locked YAG laser. The pulse and spectral widths were about 5 ps and 0.7 meV, respectively. The tunable spectral range was 350–390 nm and the average power was about 1 mW. The excitation light was incident on the sample at an angle of 30° and the luminescence was detected perpendicularly to the sample surface with a solid angle of 0.02 sr.

The detection system for the time-resolved luminescence consisted of a 75-cm double monochromator of subtractive dispersion (Narumi 750Z-1800), a synchroscan streak camera (Hamamatsu C1587), and an optical multichannel analyzer (PAR 1205A/D). The streak camera was driven directly by the electric signal from the mode locker. The time and energy resolutions of the total system were simultaneously obtained to be 15 ps and 0.5 meV, respectively, without any deconvolution. However, in order to cover a wide time interval, most of the temporal responses of the luminescence shown here were taken under the time resolution of 50 ps. The time origin was decided by detecting the diffused scattering of the excitation light from the sample surface. A part of a red light from the dye laser was fed to the streak camera directly through an optical fiber and superimposed on the luminescence signal as an absolute time-reference pulse in order to monitor a possible long-term drift of the time origin on the camera screen. Since the streak camera was scanned by a 76-MHz sinusoidal wave, an undesirable signal component delayed by about 6.6 ns was inevitably overlapped. Therefore, with the use of the signals taken at different time delays, a proper correction was made on the time responses of the luminescences with long decay times.

Owing to the high repetition rate (76 MHz), the time-resolved luminescence spectra were measured with good signal-to-noise ratio even when the peak excitation power was reduced below 10 kW/cm^2 in order to diminish high-density excitation effects. We confirmed that, for the excitation intensities up to several tens of kW/cm^2, there exist no excitation intensity dependences in the spectral shapes of both the time-integrated and the time-resolved luminescences. Therefore, our experimental condition was certainly kept in a weak-excitation regime.

III. RESULTS AND DISCUSSION

Figure 2 shows a time-integrated luminescence spectrum for an ultrapure sample taken from the excited surface (hereafter called "backward" configuration) under the excitation at 3.273 eV, which is the absorption peak energy of the $Z_{1,2}$ exciton band. Being associated with the free exciton polariton, we indicate the resonant luminescence, Ex, and its 1LO and 2LO phonon replicas, Ex-1LO and Ex-2LO, respectively, by arrows. The LO-phonon replicas are observed even up to Ex-4LO in this sample. Other luminescences in the figure are associated with crystal defects.[23] In ordinary-grade CuCl samples, Ex-1LO and Ex-2LO have been scarcely observed and the luminescence I_1 associated with an exciton bound to a neutral acceptor[24] has intensively appeared at 3.1801 eV, just on the higher-energy edge of Ex-1LO. We investigate mainly the Ex and Ex-2LO bands because of less influence from the other background luminescences.

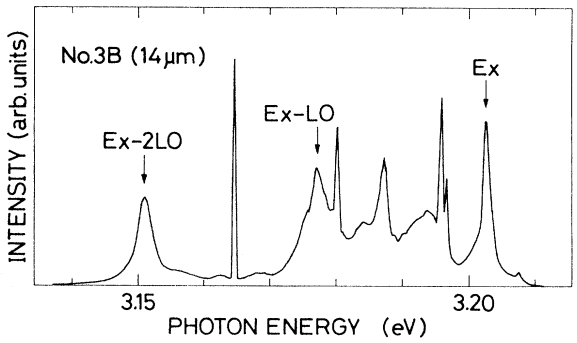

FIG. 2. Time-integrated exciton luminescence spectrum for an ultrapure CuCl single crystal at 2 K under the excitation of the $Z_{1,2}$ exciton at 3.273 eV. The resonant luminescence of Z_3 exciton polariton (Ex) and its LO-phonon replicas (Ex-LO, Ex-2LO) are indicated by arrows. The sample number and its thickness are indicated in the figure.

A. Ex-2LO luminescence

In the energy region of the Ex-2LO luminescence, the group velocity of the EP is very fast (about 6×10^{-2} of the velocity of light in vacuum) and the EP behaves "photonlike." The EP, which is observed as the Ex-2LO luminescence, has a wave vector almost normal to the surface of the slab sample and, therefore, the EP reaches the crystal surface within a time much shorter than the time resolution of 15 ps for the crystal with a thickness of ~ 10 μm. The EP immediately decays radiatively wherever the EP exists. Thus, it is valid to consider that the EP in the Ex-2LO energy region decay radiatively without any delay. Therefore, the instantaneous intensity of Ex-2LO luminescence at a certain energy should be proportional to the instantaneous number of EP's summed over the whole crystal at the energy just 2LO-phonon energy higher than the luminescence energy.[25] The effect of the LO-phonon dispersion[26] is neglected because the LO-phonon replicas are found to be located successively with a regular interval of LO-phonon energy at the Γ point[27] ($E_{LO}=26$ meV) and also because the spectral width of the Ex-2LO luminescence does not differ much from that of Ex-1LO.

Figure 3(a) shows the time-resolved spectra of Ex-2LO luminescence at different delay times after the ps pulsed excitation at the absorption peak of the $Z_{1,2}$ exciton band. At 0 ps during the pulsed excitation, Ex-2LO has a very broad shape extended well above E_T-$2E_{LO}$ (3.1502 eV) and its risetime is much shorter than the time resolution of 15 ps. Therefore, a wide energy distribution of Z_3-EP on the dispersion curve is generated from the $Z_{1,2}$ excitons through the rapid multiphonon scattering immediately after the $Z_{1,2}$-band excitation. The spectral shape of Ex-2LO, $I_{\text{Ex-2LO}}(E-2E_{LO})$, which should represent the initial energy population $N_0(E)$ of the EP having the energy E around E_T, is given by the product of the density of states $D(E)$ and a certain distribution function of the EP. Although the thermal distribution is not necessarily adequate to the initial distribution of the EP, a Boltzmann distribution function of $\exp[-(E-E_T)/k_BT]$ is adopted around the exciton resonance energy in order to get a rough estimation of an effective temperature T. In Fig. 4(a) the time-resolved Ex-2LO luminescence is shown at 0 ps (solid line) in an expanded scale and the theoretical curve (solid circles) given by

$$I_{\text{Ex-2LO}}(E-2E_{LO}) \propto N_0(E) \propto D(E)\exp[-(E-E_T)/k_BT] , \quad (3)$$

where the effective temperature T is found to be about

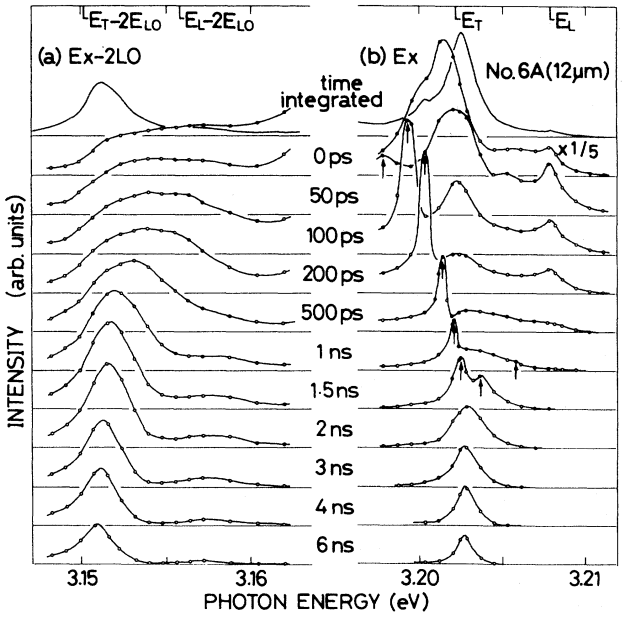

FIG. 3. Time-resolved spectra of (a) Ex-2LO and (b) Ex luminescences under the excitation of the $Z_{1,2}$ exciton. The uppermost spectrum in each column shows the time-integrated luminescence spectrum. Delay times after the ps pulsed excitation are indicated at the center. The peaks marked with vertical arrows in (b) are attributed to the coherent propagation of the EP. For details, see the text.

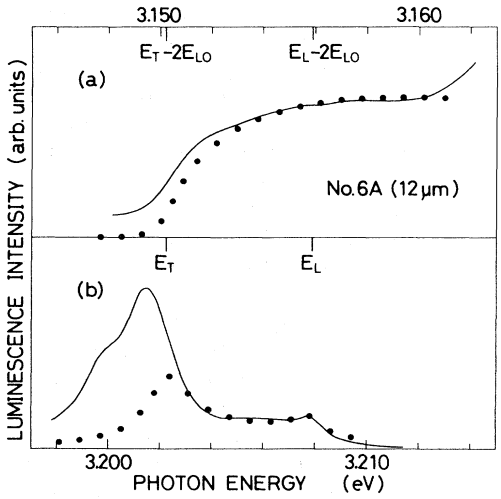

FIG. 4. Enlarged spectra of the time-resolved luminescence of Fig. 3 at 0-ps delay for (a) Ex-2LO and (b) Ex. Solid lines show experimental data and solid circles represent the theoretical curves calculated from Eqs. (3) and (4) assuming the common effective temperature of exciton polariton, $T=210$ K.

210 K. Since the thermal energy k_BT of about 18 meV is nearly equal to the energies of optical phonons and near-zone-edge acoustic phonons, the rapid relaxation of the $Z_{1,2}$ exciton into the Z_3-EP is attributed to the successive emission of optical phonons and acoustic phonons of very large wave vectors. Moreover, from the viewpoint of the density of the final states for the scattering process, the EP is considered to distribute mainly on the lower branch above E_T and much less on the upper branch even above E_L. We find no peak or structure in the Ex-2LO luminescence around E_L-$2E_{LO}$. The discrepancy in the theoretical fitting around E_T-$2E_{LO}$ indicates the deviation of the distribution function from the Boltzmann distribution together with the contribution from the background luminescence. It will be discussed further in Sec. III C.

With the lapse of time, the EP gradually relaxes toward the lower-energy side and, about 1 ns after, forms the energy distribution which has a peak at the energy a little higher than E_T as shown in Fig. 3(a). Thereafter, the peak energy shifts only slightly toward the lower-energy side and the intensity gradually diminishes. One can see the EP does not achieve the thermal equilibrium with the lattice even after 6 ns because the width of the Ex-2LO band at 6-ns delay is still much larger than the thermal energy of 0.2 meV at 2 K and the peak energy position still shows a slight lower-energy shift.

The spectrally integrated intensity of the Ex-2LO band is found to decay exponentially with the decay time of about 4 ns. It should correspond to the lifetime τ of the total number of the EP. The above-mentioned behavior of the population dynamics of the EP, in particular, the piling up of the EP population around E_T within the lifetime, is direct evidence of the "bottleneck effect" of the EP predicted by Toyozawa.[4]

The temporal responses of the Ex-2LO luminescence at

various energies are shown in Fig. 5. The observed luminescence energies are indicated on the right-hand side. On the high-energy side of the luminescence peak, the intensity rises instantaneously and decays rapidly. This decay represents the relaxation of the EP toward the lower-energy side along the lower branch dispersion curve. While, on the lower-energy side, the Ex-2LO luminescence slowly grows after the instantaneous rise and gradually decays thereafter. The decay time is extremely long for the luminescence below E_T-$2E_{LO}$ (=3.1502 eV). The instantaneous rise is ascribed to a very rapid buildup of the initial population on the lower branch through the interband relaxation from the $Z_{1,2}$ exciton band. The slow growth means the accumulation of the EP falling from the higher-energy side through the intraband slow relaxation.

B. Ex luminescence and propagation of EP

The time-resolved spectra of the Ex luminescence at different delay times are shown in Fig. 3(b). Although both of the Ex and Ex-2LO luminescences are originated from the same EP, their temporal and spectral behavior is found to be quite different due to the following reasons: (1) The group velocity of the EP in the Ex energy region is rather slow, as shown in Fig. 1(b), and it takes some finite time for the EP to reach the surface. Hence, the Ex luminescence is largely affected by the spatial distribution of the EP inside the sample. (2) The refractive index and the surface escape rate of the EP, that is, the radiative decay rate, vary significantly in the Ex energy region. Since these effects are negligible in the Ex-2LO energy region, we can observe the energy distribution of the EP directly from the Ex-2LO luminescence as already shown in Sec. III A. In the Ex energy region, on the other hand, these effects make the temporal behavior of the Ex luminescence rather complicated. However, at the same time, this fact implies that one can obtain valuable knowledge about the spatial distribution of the EP from the time-resolved Ex luminescence.

In Fig. 3(b), the Ex luminescence intensity at 0 ps is very strong, more than five times as large as the delayed one. It becomes even larger when the time resolution is improved into our best resolution of 15 ps. Moreover, as the delay time increases, strange peaks indicated by arrows are observed, which appear at different energies for different delay times. These features are more clearly understood when one observes the temporal responses of the Ex luminescence at various observation energies as shown in Fig. 6. The vertical scale in each response curve is normalized at its peak intensity. The response of the Ex luminescence has the first large peak just at 0 ps regardless of the observation energy and has the second

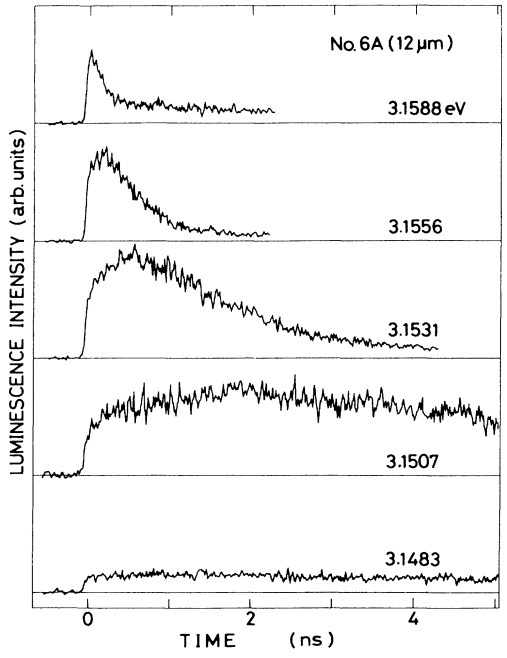

FIG. 5. Temporal responses of Ex-2LO luminescence at various observation energies under the excitation of the $Z_{1,2}$ exciton. Observation energies are indicated on the right-hand side of each curve. Luminescence intensities are comparable with one another.

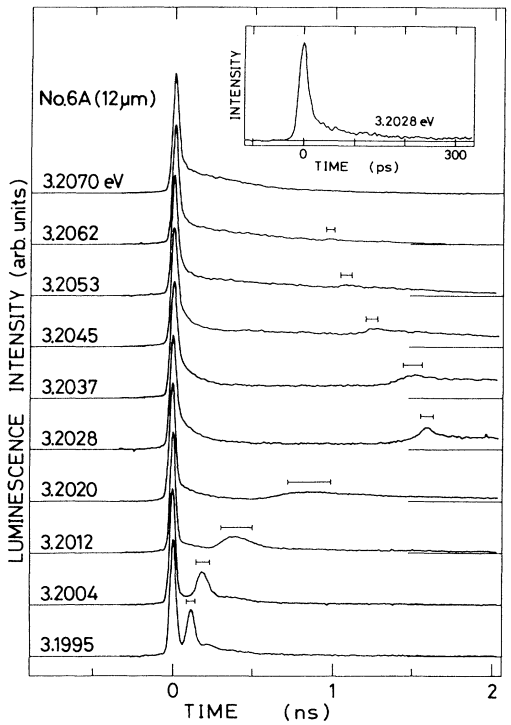

FIG. 6. Temporal responses of Ex luminescence at various observation energies under the excitation of the $Z_{1,2}$ exciton. Observation energies are indicated on the left-hand side of each curve. Luminescence intensities are normalized for the peak intensities at 0 ns. Horizontal bars approximately indicate the position and the temporal width of second peaks. The inset shows the temporal response at 3.2028 eV measured with higher temporal resolution of 15 ps.

peak at a certain delayed time depending on the observation energy. The peaks indicated by arrows in Fig. 3(b) correspond to the second peaks in Fig. 6. The delay time of the second peak from the first peak takes the maximum value at 3.2028 eV, a little higher than E_T.

We have also observed the Ex luminescence from the rear surface opposite to the excited one under the "forward" configuration. Figure 7 shows the comparison between the temporal responses of the backward and the forward Ex luminescences at 3.2028 eV. The forward luminescence is found to have a peak at a certain delayed time t_F of 800 ps, which is just a half of the delay time t_B of 1.6 ns for the second peak in the backward luminescence. The forward luminescence has almost no intensity before the delayed peak appears. The delay times t_B and t_F have been found to depend linearly on the crystal thickness d among different samples, and exactly coincide with $2d/v_g$ and d/v_g, respectively, where v_g is the group velocity of the EP at 3.2028 eV. Thus, the origin of these peak structures is evidently related to the spatial distribution and the coherent propagation of the EP.

Under the $Z_{1,2}$ excitation, the initial EP's distribute spatially only near to the excited surface because of the large absorption coefficient at the excitation energy[28] ($>10^5$ cm^{-1}) and because of the rapid conversion from the $Z_{1,2}$ exciton to the Z_3 EP through the multiphonon scattering. Therefore, the generated EP's completely lose the memory of initial wave vector of the excitation light and start to propagate isotropically from the excited surface region. They have chances to decay radiatively when they impinge on the crystal surface. However, because of the large refractive index for the lower-branch EP, the radiative decay is allowed only for EP's which propagate almost normally to the crystal surface. For example, among the EP's which propagate isotropically, only 0.6% of them can decay radiatively at E_T (=3.202 23 eV), giving the resonant luminescence Ex. The rest, that is, most of EP's, cannot contribute to the Ex luminescence and undergo the total reflection inside the crystal.

Therefore, the peaks observed in the temporal responses of the backward and the forward luminescences are well explained by the schematic illustration for the coherent propagation of EP with its group velocity as shown in the inset of Fig. 7. Among the initially generated EP's, which are populated near the excited surface, a fraction of them propagates almost normally to the excited surface, immediately reaches the excited surface, and gives a luminescence peak just after the excitation in the backward geometry. After propagating once through the crystal with the group velocity, the EP gives a luminescence peak from the rear surface for the forward geometry at the delay time $t_F(E)=d/v_g(E)$. After reflected back from the rear surface, the EP gives the second peak in the backward geometry at the delay time of $t_B(E)=2d/v_g(E)$.

According to the above assumption, the group velocity of the EP at each energy E is evaluated from the delay times $t_F(E)$, $t_B(E)$, and the sample thickness d. The group velocities obtained for different samples and geometries are shown in Fig. 8 by different symbols, together with the theoretical values by solid lines. The experimental values coincide quite well with the calculated one.

Figure 9 shows the temporal responses of the forward luminescence at various observation energies around E_L. Two peaks are found to coexist above E_L (=3.207 88 eV),

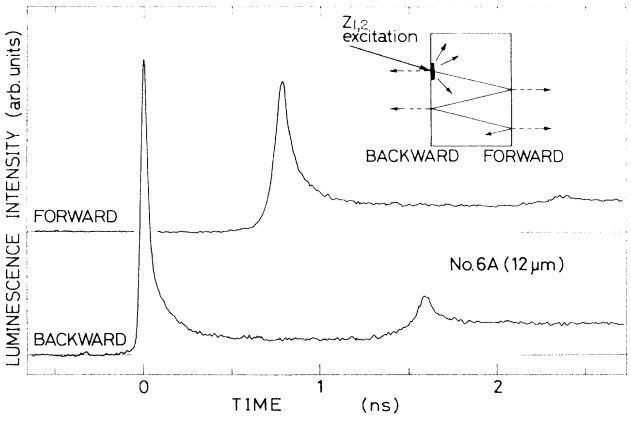

FIG. 7. Temporal responses for the backward and the forward Ex luminescences observed at the same energy of 3.2028 eV under the excitation of the $Z_{1,2}$ exciton. Intensities of the backward and the forward luminescences are calibrated to be comparable with each other. The inset shows a schematic diagram which illustrates the coherent propagation of exciton polaritons resulting in successive peaks in the temporal responses.

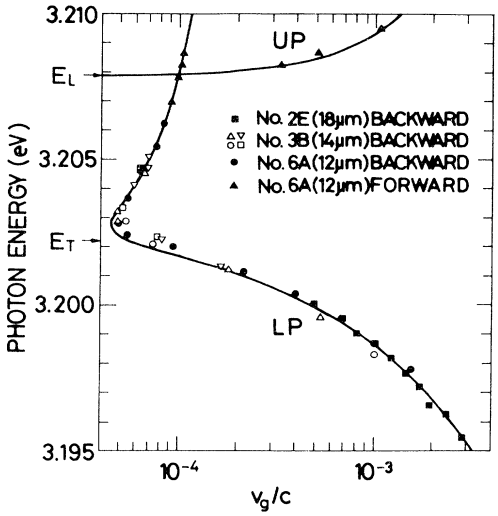

FIG. 8. Group velocities of exciton polaritons at different energies evaluated from the delay times of the peak structures which appear in temporal responses of the backward and the forward Ex luminescences for various samples. Solid lines show theoretical curves calculated from Eqs. (1) and (2). LP and UP denote the lower-branch polariton and the upper-branch polariton, respectively.

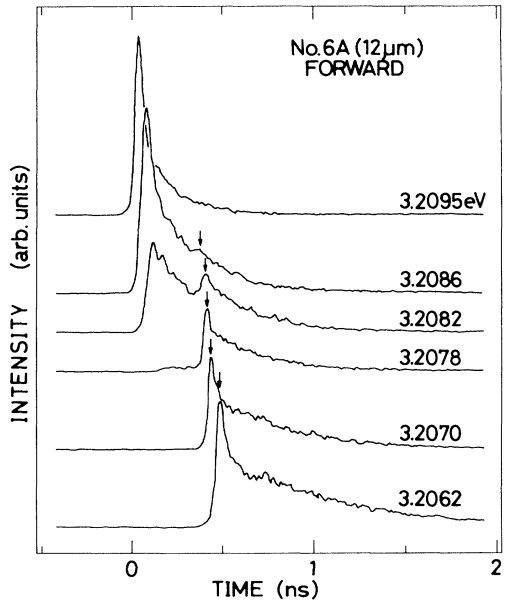

FIG. 9. Temporal responses of the forward Ex luminescence at various observation energies around E_L (=3.207 88 eV) under the excitation of the $Z_{1,2}$ exciton. Observation energies are indicated on the right-hand side of each curve. Two peaks coexist around E_L, where the earlier peak comes from the upper-branch polariton and the later one indicated by an arrow comes from the lower-branch polariton.

where the earlier peak comes from the upper-branch EP and the later one indicated by an arrow comes from the lower-branch EP. Since the scattering rate of the EP increases toward the higher-energy side, as we will discuss later in Sec. III E, most of the lower-branch EP's having very slow group velocities around E_L should be scattered out before their arrival at the rear surface. Furthermore, the escape rate of the EP at the sample surface for the upper-branch EP should be much larger than that for the lower-branch EP. Nevertheless, the intensities of the two peaks are comparable. This fact firmly supports that the photogenerated EP's initially distribute mostly on the lower branch as discussed in Sec. III A. The coexistence of the upper-branch EP and the lower-branch EP is observed within 1 meV above E_L. This coexistence has never been observed in previous time-of-flight measurements because the initial population ratio of the lower-branch EP to the upper-branch EP is considered to be much less than the ratio in our case, since the former ratio is related only to the additional boundary condition in the usual time-of-flight measurement.[10]

Next, we discuss the widths of the peak structures in Fig. 6. For the first peak just after the excitation in the backward luminescence, the width is found to be mainly limited by our time resolution. We show the temporal response at 3.2028 eV with our best time resolution of 15 ps in the inset of Fig. 6. Since, at the first moment just after the excitation, the EP's start to propagate coherently with their group velocity, the temporal response of the first peak depends on the initial spatial distribution of the EP. The initial spatial distribution of the EP at the depth z from the excitation surface is proportional to $\alpha \exp(-\alpha z)$, where α is an absorption coefficient at the excitation energy. Therefore, the first peak should decay with the form of $\exp(-\alpha v_g t)$. The time constant $(\alpha v_g)^{-1}$ is equal to or less than 3 ps under the $Z_{1,2}$ excitation with the absorption coefficient[28] $\alpha \simeq 3\times 10^5$ cm^{-1}. It is much less than our time resolution. The validity of the above discussion has been further confirmed by the experimental fact that the decay of the first peak is dependent on α when we change the excitation energy away from the $Z_{1,2}$ absorption peak. The details will be published elsewhere.

On the other hand, the widths of the second peak in the backward luminescence and the first peak in the forward luminescence are attributed to the dispersion of the group velocity; that is, the second derivative of the EP energy with respect to the wave vector because of the finite spectral resolution for the observation. The measured peak position with its half-width is shown in Fig. 6 by a horizontal bar on each curve, which explains quantitatively how the peak broadening changes. The width is most diffused around 3.2020 eV, a little below E_T, where the group velocity changes most significantly.

Finally, we discuss the background luminescence other than the peak structures in Fig. 6. It is caused by the incoherent motion of the EP's which are scattered more than once through the momentum relaxation and reach the surface after random delay times. The background intensity is not so important as compared with the first peak in the temporal response of the backward spectra. This fact suggests a rather slow intraband relaxation rate of the EP along the dispersion curve in the measured energy region in Fig. 6. However, for the time-integrated luminescence intensity, the "background" component has significant contribution as shown in Fig. 3(b). After the delay time of 2 ns, the Ex luminescence almost loses its fine structures and the luminescence shape becomes similar to that of the Ex-2LO luminescence as shown in Figs. 3(a) and 3(b). This result indicates that most of the EP's have already experienced the intraband scattering within 2 ns, and therefore, the spatial inhomogeneity of the EP distribution has been almost inconspicuous.

C. Ex luminescence at 0 ps delay

As mentioned above, the EP's generated indirectly propagate coherently with their group velocity and a part of them decay radiatively when they impinge on the crystal surface. Therefore, the line shape of the time-resolved resonant luminescence is largely governed by such kinetics of the EP. However, at 0-ps delay, all the EP's distribute only near the crystal surface. Therefore, the line shape of Ex luminescence at 0 ps is expected to directly reflect the initial energy distribution of the lower-branch EP. Taking into account the rapid change of the surface reflectivity, the refractive index, and the group velocity around E_T, the line shape is expressed as

$$I_{\mathrm{Ex}}(E) \propto \frac{1}{[n_L(E)]^2} P(E) \int_0^{v_g(E)\Delta t} N_0(E) e^{-\alpha z} dz \ , \quad (4)$$

where $n_L(E)$ and $P(E)$ are the refractive index equal to $\hbar ck/E$ and the surface escape probability of the lower-branch EP at the energy E, respectively. The first factor of $1/[n_L(E)]^2$ enters due to the requirement of a fixed outside solid angle for the observation.[29] The integral part is simply proportional to $N_0(E)$ because the time resolution Δt is much larger than $[\alpha v_g(E)]^{-1}$ as discussed in Sec. III B. For the evaluation of the escape probability $P(E)$, the conversion of the EP from the lower branch to the upper branch on the occasion of the inward reflection at the crystal surface is not considered because the conversion probability is much less than the inside reflectivity $R_L(E)$ for the lower-branch EP. Therefore, we approximately put $P(E)=1-R_L(E)$. The value $R_L(E)$ is calculated with the use of the ordinary electromagnetic boundary conditions and Pekar's additional boundary condition,[30,31] and the result is shown by a dashed line in Fig. 1(b). The change in the reflectivity $R_L(E)$ other than the normal incidence is also neglected because the inside solid angle for the observation is small enough. With the adoption of $N_0(E)$ in the form of Eq. (3) for $T=210$ K, the calculated line shape is shown in Fig. 4(b) by dotted circles. It accounts well for the experimental one (solid line) above E_T when the theoretical value is fit to the experimental one at E_L. It should be noticed that the peak at E_L comes from the contribution, not of the upper-branch EP often referred to,[32,33] but of lower-branch EP associated with an anomaly in the reflectivity R_L around E_L.[30] Below E_T, the observed luminescence intensity is much larger than the calculated one. In particular, there exists a shoulder around 3.200 eV, which may be caused by the direct generation of the EP at this energy region through 2LO+TO or 2LO+LA+TA phonon[27] emission when the $Z_{1,2}$ excitons are excited. The initial distribution around this energy region is, therefore, somewhat different from the simply assumed Boltzmann distribution. The effect of deviation from the Boltzmann distribution is strikingly large on the Ex luminescence below E_T where the escape rate of the EP is very large compared with that above E_T, while it is not so significant on the total population of the EP which is represented only by the lower-energy tail part of the Ex-2LO luminescence below E_T-$2E_{LO}$ as shown in Fig. 4(a).

D. Sample dependence of time-integrated luminescence spectra

The line shapes and the intensities of the Ex-2LO and Ex luminescences in the time-integrated spectra are found to depend strongly on the sample quality due to the competitive relation between the lifetime and the intraband relaxation time of the EP. Figure 10 shows an example of the time-integrated luminescence spectra under the excitation of the $Z_{1,2}$ exciton band for three different samples with the same thickness. The lifetime of the EP, τ, varies from 4 ns to less than 0.5 ns in these samples and is indicated on the left-hand side of each curve. The absolute intensity of the Ex luminescence decreases from Figs. 10(a) to 10(c), although the luminescence intensity is normalized for the peak intensity of the

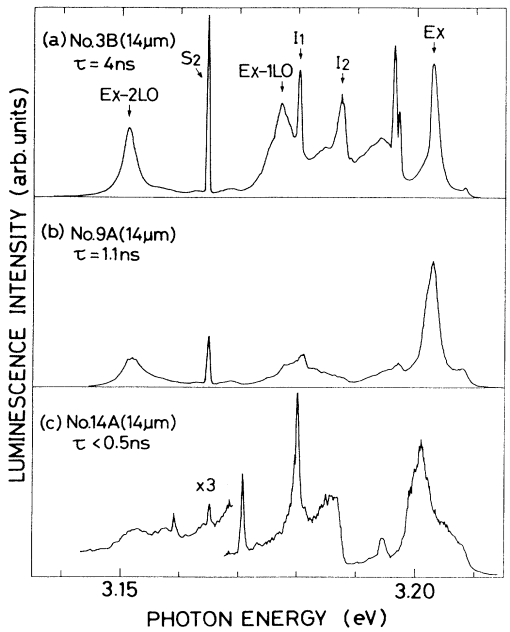

FIG. 10. Time-integrated luminescence spectra in three different samples with the same thickness under the excitation of the $Z_{1,2}$ exciton. The lifetime τ for the total number of exciton polaritons in each sample is indicated on the left-hand side of each curve, which is evaluated from the decay time of the spectrally integrated intensity of Ex-2LO luminescence.

Ex luminescence. For highly pure samples in which the lifetime of the EP is longer than 2 ns, the Ex-2LO band is clearly observed as an intense peak as shown in Fig. 10(a). The line shape of Ex-2LO is very sharp and does not have any asymmetric tail toward the higher-energy side which has been usually attributed to the thermal distribution of excitons at a certain effective temperature.[25] On the other hand, for our ordinary samples in which the lifetime of the EP is about 1 ns, the Ex-2LO band is found to be weak compared to the Ex luminescence and has a broad tail on the higher energy side as shown in Fig. 10(b). For the worse samples, with the lifetime of the EP much less than 1 ns, it is difficult to distinguish the Ex-2LO luminescence from the background luminescence because of the excess broadening and the weak intensity as shown in Fig. 10(c). These changes in the Ex-2LO line shape are well explained by the difference in the degree of intraband energy relaxation of the EP within the lifetime that is well illustrated in the time-resolved spectra of the Ex-2LO luminescence shown in Fig. 3(a) for a highly pure sample.

On the other hand, the Ex luminescence behaves somewhat differently. Two characteristic features should be noticed: One is the energy position and the width of the main peak around E_T, and the other is the intensity ratio of the subpeak at E_L to the main peak. These features are explained again by the time-resolved spectra shown in Fig. 3(b). The subpeak appears only at an early stage after the pulsed excitation because of the intraband relax-

ation toward the low-energy side. The main band becomes sharper and locates around E_T after the delay time of 1 ns. Therefore, as the lifetime of EP increases from Figs. 10(c) to 10(a), the intensity ratio of the subpeak to the main peak becomes small, the main peak position shifts to E_T, and the width of the main peak becomes sharp. However, the effect of sample quality on the Ex luminescence is less distinct compared with the Ex-2LO luminescence because the Ex luminescence under the $Z_{1,2}$ band excitation is the strongest just after the excitation.

Therefore, one can recognize the order of magnitude for the EP lifetime, in other words, the quality of the samples from the spectral line shapes of both the Ex and Ex-2LO luminescences in addition to their absolute intensities. It is noticed from the comparison among the spectra in Fig. 10 that the intensity ratio of Ex luminescence to other extrinsic bound exciton luminescences such as I_1 and I_2 is not always a good indication for the quality of the sample. We have found no definite correlation between the EP lifetime and the intensity of extrinsic luminescences in our CuCl samples.

E. Evaluation of scattering rate

Figure 6 shows that the intensity of the second peak in the temporal response of the backward Ex luminescence decreases with increasing the observation energy above E_T and finally diminishes near E_L. The decrease of the second peak intensity implies the existence of scatterings of the EP during the propagation inside the sample. In order to evaluate the scattering rate at an energy E, we assume the following situation for the dynamics of the EP: At the crystal surface, the lower-branch EP impinging perpendicularly on the crystal surface is reflected back with the inside reflectivity $R_L(E)$ and escapes from the crystal surface as the radiative decay with the probability $P(E)$. After the propagation by a distance of the sample thickness d, the EP keeping the initial coherent motion survives with the probability $T(E)$ which corresponds to an inside transmissivity. When the EP's are initially generated close to the front excited surface, one-half of them start to propagate toward the front surface and the rest toward the rear surface. Thus, the intensity of each peak appearing in the forward or the backward luminescences is calculated as follows, except for a common factor: For the first peak in the backward geometry,

$$I_{B1}(E)=P(E) , \tag{5a}$$

for the first peak in the forward geometry,

$$I_{F1}(E)=[1+R_L(E)]T(E)P(E) , \tag{5b}$$

and for the second peak in the backward geometry

$$I_{B2}(E)=[1+R_L(E)]R_L(E)[T(E)]^2P(E) . \tag{5c}$$

Then the inside transmissivity $T(E)$ is given as

$$T(E)=\frac{1}{1+R_L(E)}\frac{I_{F1}(E)}{I_{B1}(E)} \tag{6a}$$

or

$$T(E)=\left[\frac{1}{[1+R_L(E)]R_L(E)}\frac{I_{B2}(E)}{I_{B1}(E)}\right]^{1/2} . \tag{6b}$$

Since the peak structures are broadened due to the dispersion of the group velocity as mentioned earlier, one should evaluate energy-dependent values of $T(E)$ from the ratio of the integrated intensities of the peak structures with respect to time. The energy dependence of $T(E)$ is shown in Fig. 11, where open triangles and open circles are calculated from Eqs. (6a) and (6b), respectively. Since the optical configurations are different between the backward and the forward luminescences, the absolute value of $I_{F1}(E)/I_{B1}(E)$ is not exactly obtained. Therefore, an adjustable factor is introduced for $T(E)$ in Eq. (6a) so as to fit with the absolute value of $T(E)$ obtained from Eq. (6b) around 3.204 eV.

Below E_T, $T(E)$ is almost unity and, therefore, the EP is scarcely scattered during the one-round-trip time. In this energy region, as well as the small scattering rate, the reduction of the transit time through the sample due to the rapid increase of the group velocity mainly contributes to get $T(E)\simeq 1$. On the other hand, $T(E)$ decreases with the increase of energy above E_T. The decrease of $T(E)$ mainly represents the increase of the scattering rate of the EP in this energy region because the group velocity of the EP changes only slightly above E_T. By introducing the scattering probability of the EP per unit time, $\tau_m^{-1}(E)$, $T(E)$ is transformed to $\tau_m^{-1}(E)$ as

$$\tau_m^{-1}(E)=-\frac{v_g(E)}{d}\ln[T(E)] . \tag{7}$$

The energy dependence of the scattering probability $\tau_m^{-1}(E)$ thus obtained is shown in Fig. 12. Below 3.2023 eV, meaningful values cannot be obtained because of large error bars in $T(E)$. The scattering probability is about 10^9 s^{-1} just above E_T. It increases with the in-

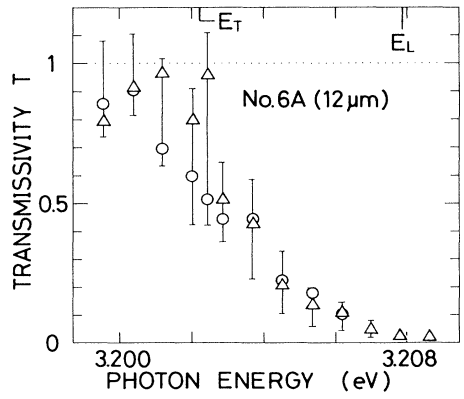

FIG. 11. Inside transmissivity $T(E)$ of the lower-branch exciton polariton for one transit through the sample thickness of 12 μm. Circles and triangles denote the inside tranmissivities evaluated from the backward and the forward Ex luminescences, respectively.

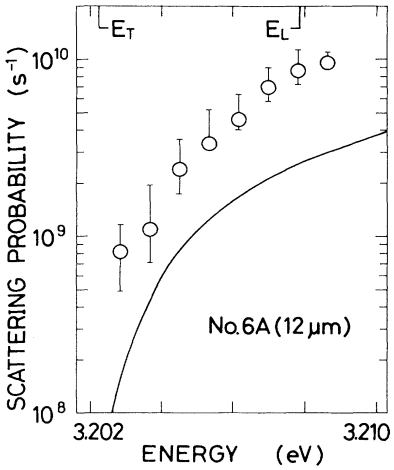

FIG. 12. Scattering probability per unit time (momentum-relaxation rate) τ_m^{-1} of the lower-branch exciton polariton shown by open circles, which is evaluated from the inside transmissivity $T(E)$. Solid line represents the inelastic-scattering probability of exciton polariton theoretically obtained for the one-LA-phonon emission at 2K.

crease of energy and reaches 10^{10} s^{-1} around E_L. Since the intraband relaxation of the EP toward the lower-energy side is observed in the Ex-2LO luminescence as shown in Fig. 3(a), the obtained scattering probability is expected to contain the contribution from the scattering of the EP by an acoustic phonon emission. The contribution from the nonradiative decay process is negligible in these values since the lifetime of the total number of the EP ($\tau \simeq 4$ ns) is much longer than the scattering time τ_m. The acoustic phonon scattering in CuCl is considered to be dominantly caused through the interaction of deformation potential type.[7] A solid line in Fig. 12 shows the scattering probability of the EP at 2 K by one-LA-phonon emission which is calculated from the formula given by Toyozawa,[3] with taking the EP dispersion into account.[22] The deformation potential of the exciton is taken to be -0.4 eV.[34] The scattering probability experimentally obtained has an energy dependence similar to the theoretical one, but the absolute value differs by a factor of about 3.

Here, we should examine what kind of scattering processes we have observed: inelastic scattering or an elastic one. In ordinary discussion on luminescence spectra, the existence of elastic scattering is not considered because one only restricts the photon energy of the luminescence by the use of a monochromator. However, the wave-vector direction of the EP is also restricted by the observation of the EP luminescence since the radiative decay is allowed only for the specific EP which has the wave vector normal to the crystal surface. Therefore, not only the inelastic scattering but also the elastic scattering contribute to make $T(E)$ small. Namely, the obtained scattering probability represents the momentum-relaxation probability; that is, the sum of the inelastic-scattering probability and the elastic one. As far as we know, this is the first observation of the momentum-relaxation probability in exciton-polariton systems using the time-resolved spectroscopy. As already reported briefly in Ref. 22, we have succeeded in the direct measurement of the energy-relaxation probability of the EP per unit time under the Z_3 resonant excitation and found that the energy-relaxation probability almost coincides with the calculated acoustic-phonon scattering probability. Therefore, we conclude that the momentum-relaxation probability contains the elastic scattering by crystal imperfections together with the inelastic scattering by the acoustic-phonon emission. The results and quantitative discussion will be published elsewhere.

Recently, Kuwata *et al.*[35] have independently reported the similar pulsed response of the Ex luminescence in a CuCl sample with a thinner thickness of 2.6 μm and they have claimed that the EP's propagate with the group velocity without any intraband relaxation. However, if the EP were free from the intraband scattering, multiple peaks should appear successively in the temporal responses for the energy region between E_L and E_T (L-T splitting region) because of the high reflectivity. The absence of the successive peaks in their data definitely shows the existence of scattering process and/or nonradiative decay process. Using the same procedure described in this section, we have estimated the scattering probability of the EP in their sample to be about 10^{10} s^{-1} with little energy dependence inside the L-T splitting region. Thus, we surmise that the extrinsic scattering or trapping of the EP is too frequent in their sample to observe the slow intraband scattering.

We have also found the sample dependence of the scattering probability in our samples. Among the samples shown in Fig. 10, the intensity of the second peak in the backward Ex luminescence depends on the lifetime of the EP and in sample No. 14A the second peak is not detectable at all in the L-T splitting region even though the sample thickness of 14 μm is equal to that of sample No. 3B.

Finally, we examine the assumption that no damping is included in the dispersion relation [Eq. (1)]. The damping Γ (full width at half maximum for Lorentzian broadening of the EP) should be connected with the momentum-relaxation probability τ_m^{-1} by $\Gamma = \hbar/\tau_m$. Then the magnitude of Γ is found to be 0.01 meV at most around E_L, and therefore, we reconfirm that the dispersion relation is scarcely modified by the damping process in our highly pure samples.

F. Comparison of the inside transmissivity $T(E)$ with the transmission spectra

By using the inside transmissivity $T(E)$, we reproduce the ordinary transmission spectrum $T_{out}(E)$ below E_L as

$$T_{out}(E) = \frac{[1-R_L(E)]^2 T(E)}{1-[R_L(E)T(E)]^2} , \tag{8}$$

where the multiple reflection inside a slab sample is taken into account except for the interference. The inside

reflectivity of the lower-branch EP, $R_L(E)$, and the outside reflectivity of the incident light are identical below E_L. The minimum value of $T(E)$ of 2×10^{-2} just below E_L leads to the minimum value of $T_{out}(E)$ of 5×10^{-3}. However, this value is unexpectedly large compared with the transmissivity of less than 10^{-4}, which is experimentally obtained for the same sample in an ordinary transmission measurement. It is also found that the absolute intensity and the line shape of the transmission spectra in the L-T splitting region vary considerably from sample to sample even though the lifetime of the EP and the thickness of the sample are not much different. This result suggests the existence of extrinsic origins for the reduction of transmitted light intensity, together with the momentum relaxation of the EP inside the sample.

In order to explain the discrepancy between $T_{out}(E)$ and the transmission spectrum, we propose the effect of fine surface roughness of the order of 10 nm, although there are only a few papers which deal with the optical effects of the surface roughness of the semiconductor crystal.[36] In the L-T splitting region, the refractive index for the lower-branch EP well exceeds 10, and therefore, even a small roughness of the crystal surface which is hardly detectable for ordinary light may refract the outgoing light quite diffusively. The transmitted light is so diffused that the intensity of the transmitted light collected in a small limited solid angle becomes very weak. Furthermore, the slight deviation from the perfect parallelism between the front and rear surfaces may deflect the beam direction severely around the L-T splitting region. We have experimentally observed the strong diffusion and the deflection of the transmitted light beam inside the L-T splitting region in CuCl by observing the beam profile with the use of a TV camera. The results will be published elsewhere. These facts indicate the difficulty of obtaining the scattering probability of the EP directly from the transmission spectra in the exciton resonance region[37] unless one carefully chooses slab samples having very smooth and parallel surfaces.

Here, it is noticed that in our measurement of the Ex luminescence, the effect of the surface roughness is fortunately removed because the EP propagates isotropically from the first moment. If the roughness is random enough and is treated statistically, the diffused transmission (or luminescence) light beams compensate one another in intensity on the outside of the crystal. Although the roughness also affects the internal reflection, the small roughness is not so effective even in the region of a large refractive index as in the case of transmission. Therefore, our measurement is considered to give the right value for the inside transmissivity free from the surface roughness.

Because of the false values of the transmissivity obtained from the conventional transmission measurement, many researchers have not noticed the importance of the coherent propagation of the EP in the L-T splitting region. That seems to be one of the reasons why they could not notice the new aspects of the EP luminescence dynamics mentioned in this paper.

IV. CONCLUSIONS

We have observed ps time-resolved luminescences of Z_3 exciton polariton in ultrapure CuCl single crystals at 2 K under the excitation of the $Z_{1,2}$ exciton band in the condition of weak-excitation regime. We have found the following facts: First, the energy distribution of the EP is directly measured by the observation of the 2-LO-phonon replica "Ex-2LO." Under the $Z_{1,2}$ excitation, the wide energy distribution of Z_3 EP is initially generated through the multiphonon emission instantaneously within our time resolution of 15 ps. After the lapse of time of about 1 ns, the EP shows the energy relaxation toward the lower-energy side with almost no decay in their population number. The distribution of the EP piles up at around E_T and shows the "bottleneck effect." However, the EP does not achieve the thermal equilibrium with the lattice temperature within its lifetime. The lifetime of the EP is obtained from the temporal behavior of the spectrally integrated Ex-2LO luminescence. It amounts to 4 ns in some samples.

Second, the temporal and spectral shapes of the EP resonant luminescence, "Ex," are found to be governed by the spatial distribution of the EP inside the sample since the EP's propagate coherently and give the resonant luminescence only when they impinge on the sample surfaces. The initial spatial distribution is localized along the narrow region near the excited surface due to the strong absorption of the excitation light. The temporal responses of the Ex luminescence are different between the measurements from the excited surface and from the opposite surface. In both of the temporal responses, peak structures are observed which reflect the temporal change of the spatial distribution of the EP by the coherent propagation of the EP with its group velocity. It is shown that the EP at the exciton resonance energy propagates coherently for a distance of more than 20 μm at 2 K, provided the sample is pure enough.

Third, the momentum-relaxation probability of the EP and its energy dependence within the energy region between E_T and E_L of the Z_3 exciton are obtained from the ratio of the intensities of the peak structures in the temporal responses of the Ex luminescence. The scattering probability per unit time is about 10^9 s^{-1} around E_T, increases with the increase of energy, and reaches 10^{10} s^{-1} around E_L. The momentum-relaxation probability contains both elastic and inelastic scatterings. The inelastic scatttering is caused by the acoustic-phonon emission which is clearly observed as the intraband energy relaxation in the Ex-2LO luminescence, and the elastic scattering is presumably caused by the crystal imperfections.

ACKNOWLEDGMENTS

The authors wish to thank Professor T. Goto, Professor K. Cho, and Dr. Y. Nozue for fruitful discussions and valuable suggestions. This work is partially supported by a Grant-in-Aid for Scientific Research from the Ministry of Education, Science and Culture.

[1]J. J. Hopfield, Phys. Rev. **112**, 1555 (1958).
[2]S. I. Pekar, Zh. Eksp. Teor. Fiz. **34**, 1176 (1958) [Sov. Phys. JETP **7**, 813 (1958)].
[3]Y.Toyozawa, Prog. Theor. Phys. **20**, 53 (1958).
[4]Y. Toyozawa, Prog. Theor. Phys. Suppl. **12**, 111 (1959).
[5]H. Sumi, J. Phys. Soc. Jpn. **41**, 526 (1976).
[6]P. Wiesner and U. Heim, Phys. Rev. B **11**, 3071 (1975).
[7]Y. Masumoto and S. Shionoya, J. Phys. Soc. Jpn. **51**, 181 (1982).
[8]Y. Masumoto and S. Shionoya, Phys. Rev. B **30**, 1076 (1984).
[9]Y. Segawa, Y. Aoyagi, K. Azuma, and S. Namba, Solid State Commun. **28**, 853 (1978).
[10]Y. Masumoto, Y. Unuma, Y. Tanaka, and S. Shionoya, J. Phys. Soc. Jpn. **47**, 1844 (1979).
[11]I. Filinski, Nuovo Cimento B **39**, 533 (1977).
[12]C. Hermann and P. Y. Yu, Phys. Rev. B **21**, 3675 (1980).
[13]J. Lee, E. S. Koteles, M. O. Vassell, and J. P. Salerno, J. Lumin. **34**, 63 (1985).
[14]J. Aaviksoo, A. Freiberg, J. Lippmaa, and T. Reinot, J. Lumin. **37**, 313 (1987); J. Aaviksoo, *ibid.* **48/49**, 57 (1991).
[15]Y. Nozue and T. Goto, J. Phys. Soc. Jpn. **58**, 1831 (1989).
[16]G. W.'t Hooft, W. A. J. A. van der Poel, L. W. Molenkamp, and C. T. Foxon, Phys. Rev. B **35**, 8281 (1987).
[17]H. Hillmer, A. Forchel, S. Hansmann, M. Morohashi, and E. Lopez, Phys. Rev. B **39**, 10 901 (1989).
[18]T. C. Damen, J. Shar, D. Y. Oberli, D. S. Chemla, J. E. Cunningham, and J. M. Kuo, Phys. Rev. B **42**, 7434 (1990).
[19]T. Itoh, T. Katohno, T. Kirihara, and M. Ueta, J. Phys. Soc. Jpn. **53**, 854 (1984).
[20]T. Mita, K. Sotome, and M. Ueta, Solid State Commun. **33**, 1135 (1980).
[21]T. Itoh, J. Fashan, Y. Iwabuchi, and T. Ikehara, in *Ultrafast Phenomena VI,* edited by T. Yajima, K. Yoshihara, C. B. Harris, and S. Shionoya (Springer-Verlag, Berlin, 1988), p. 252.
[22]T. Ikehara and T. Itoh, in *Proceedings of the 20th International Conference on the Physics of Semiconductors, Thessaloniki, 1990,* edited by E. M. Anastassakis and J. D. Joannopoulos (World-Scientific, Singapore, 1991), p. 1943.
[23]M. Ueta, T. Goto, and T. Yashiro, J. Phys. Soc. Jpn. **20**, 1022 (1965).
[24]M. Certier, C. Wecker, and S. Nikitine, J. Phys. Chem. Solids **30**, 2135 (1969).
[25]V. A. Abramov, S. A. Permogorov, B. S. Razbirin, and A. I. Ekimov, Phys. Status Solidi **42**, 627 (1970).
[26]Z. Vardeny, G. Gilat, and A. Pasternak, Phys. Rev. B **11**, 5175 (1975).
[27]T. Fukumoto, S. Nakashima, K. Tabuchi, and A. Mitsuishi, Phys. Status Solidi B **73**, 341 (1976).
[28]Y. Kato, T. Goto, T. Fujii, and M. Ueta, J. Phys. Soc. Jpn. **36**, 169 (1974).
[29]Y. Nozue, J. Phys. Soc. Jpn. **57**, 3204 (1988).
[30]F. Askary and P. Y. Yu, Solid State Commun. **47**, 241 (1983).
[31]K. Cho and M. Kawata, J. Phys. Soc. Jpn. **54**, 4431 (1985).
[32]D. D. Sell, S. E. Stokowski, R. Dingle, and J. V. DiLorenzo, Phys. Rev. B **7**, 4568 (1973).
[33]S. Suga and T. Koda, Phys. Status Solidi B **66**, 255 (1974).
[34]J. B. Anthony, A. D. Brothers, and D. W. Lynch, Phys. Rev. B **5**, 3189 (1972).
[35]M. Kuwata, T. Kuga, H. Akiyama, T. Hirano, and M. Matsuoka, Phys. Rev. Lett. **61**, 1226 (1988).
[36]V. A. Kosobukin and A. V. Sel'kin, Solid State Commun. **66**, 313 (1988).
[37]I. Broser, K.-H. Pantke, and M. Rosenzweig, Solid State Commun. **58**, 441 (1986).